International Journal on Engineering Applications (I.R.E.A.), Vol. 13, N. 4
ISSN 2281-2881 July 2025

Numerical Study of Advanced Sail Design Optimization Based on Environmental Conditions Towards Energy Efficiency Design Index (EEDI)

Betty Ariani[1], Ponidi[2], M. Arif Batutah[2], Ardan Nagra Coutsar[3]

Abstract – *The demand for maritime transportation has increased significantly over the past two decades, accompanied by the rise of green technology interventions aimed at improving energy efficiency, reducing emissions, and lowering operational costs. The International Maritime Organization (IMO) has implemented new regulations limiting CO_2 emissions through the Energy Efficiency Design Index (EEDI). These regulations necessitate precise technological adaptations. This study investigates the application of rotor sail technology, which harnesses wind power to provide additional thrust to vessels. Numerical studies using Computational Fluid Dynamics (CFD) simulations have been conducted with rotor heights of 20, 25, and 30 meters under wind speeds of 5, 10, and 15 m/s. EEDI analysis has been performed for four vessel types, 50,000, 100,000, 150,000, and 200,000 DWT, with and without rotor sails. The results demonstrate that implementing sail technology significantly enhances the energy efficiency of vessels, as evidenced by a reduction in the EEDI across various vessel types and wind speeds. Efficiency improvements are particularly pronounced at higher wind speeds, highlighting the advantages of sails in favorable conditions. Additionally, larger vessels experience greater efficiency gains when utilizing sail technology. These findings underscore the potential of sail technology to reduce emissions and support the sustainability of maritime operations.*

***Keywords**: Advanced Sail, Carbon Emissions, Energy Efficiency, Rotor, Wind Energy*

Nomenclature

IMO	International Maritime Organization
CO_2	Carbon dioxide
EEDI	Energy Efficiency Design Index
CFD	Computational Fluids Dynamic
DWT	Dead Weight Tonnage
SEEMP	Ship Energy Efficiency Management Plan
GHG	Green House Gases
HFCs	Hydrogen Fuel Cells
NO_x	Nitroxide
SO_x	Sulfur oxide
LNG	Liquefied Natural Gases
PM	Particulate Matter
FOC	Fuel Oil Consumption

I. Introduction

The growing demand for goods transportation and human mobility has become a key factor driving the development of transportation infrastructure. According to data from Mamun et al, 2016 [1], sea transportation is currently the most widely relied-upon mode of transport.

Data presented by Johnson, 2014 [2], indicates that approximately 90% of global freight is transported via sea routes. This surge in maritime traffic has inevitably led to a proportional increase in fuel demand. The predominant reliance on fossil fuels in ships has positioned the shipping industry as a significant contributor to global emissions, accounting for approximately 3% of the worldwide greenhouse gas emissions [3]. Furthermore, fuel consumption represents a critical issue as it directly influences operational costs, which in turn affect transportation rates. Despite this, ships remain a preferred mode of transport due to relatively low shipping costs. In response to these challenges, the emphasis on fuel efficiency has intensified, driving efforts to adopt alternative fuels for maritime vessels. The International Maritime Organization (IMO) has implemented several policies to address emissions, including the Energy Efficiency Design Index (EEDI) and the Ship Energy Efficiency Management Plan (SEEMP) [4], [5]. These measures aim to reduce Greenhouse Gas (GHG) emissions, ultimately striving for zero carbon emissions.

Greenhouse gases are the primary drivers of global warming, which is projected to increase global temperatures by 3 to 5 °C by 2050. If left unchecked, this warming could lead climate change that threatens the very existence of life on Earth. Global efforts to reduce emissions from the maritime transport sector are crucial for addressing climate change challenges and ensuring the sustainability of both the global economy and ecosystems

 https://doi.org/10.15866/irea.v13i4.25693

[6]. The discourse on the use of renewable energy is broadly expected to serve as a tangible effort to reduce GHG emissions. However, as noted by Saavendra et al. (2021) [7], the implementation of renewable energy technologies requires significant investment, which makes it less competitive compared to traditional fossil fuels. In the maritime sector, green technology interventions, particularly through the applications of alternative fuels, have emerged as a pivotal strategy for enhancing energy efficiency and reducing emissions. Various alternative fuels and systems under development for shipping include solar cell technology, natural gas, wind-assisted propulsion, hydrogen, biofuels, and others. Dolatadi et al, 2023 [8], studied a hybrid system combining green hydrogen, wind energy, and solar power for bulk carriers.

The findings indicate that wind power, solar energy, and Hydrogen Fuel Cells (HFCs) could contribute 8 to 27%, less than 1%, and 50 to 100% of the total propulsion power, respectively, depending on specific operational parameters. Similarly, the research by Tuswan et al., 2023 [9], explored the potential of natural gas in reducing greenhouse gases emissions from ships.

Their study demonstrated that Liquefied Natural Gas (LNG) could lower NOx, SOx, and Particulate Matter (PM) emission factors by 86.1%, 94.5%, and 92.7%, respectively, compared to conventional fossil fuels. Dual-fuel diesel-natural gas engines have been identified as the most practical option due to their operational flexibility.

However, methane slip remains as a significant drawbacks, as highlighted by Ariani et al, 2019 [10] Regarding biofuels, [11], [12] have shown that their application in the shipping industry has not yet provided substantial support for achieving net-zero emissions. Biofuel usage has not yet become a supportive force for the transport industry in achieving net-zero emissions.

While biofuels hold promise, their implementation is constrained by challenges such as land use requirement for production, which could negatively affect the environment. Several methods used to reduce a vessel's Energy Efficiency Design Index (EEDI) include the application of sail technology to harnesses wind power for additional thrust [13], and optimizing the vessel's design to minimize hydrodynamic resistance through streamlined shapes and sizes. M.S Calisal et al., 2022, used The Pareto Frontier technique for multi-objective optimization of ship dimension parameters in design, viewed from the perspective of EEDI [14]. Y. H. Hou et al., 2018 studied the adaptability and the reliability of hull line design influences for achieving minimum EEDI incorporating Design of Experiments (DoE) and Reliability-Based Optimization Design (RBOD) [15]. H. Ren et al, 2019, studied and analysed engine-propeller matching and EEDI, by focusing on parameters such as ship speed, effective power, and propeller diameter [16]. Y. Hang Hou et al., 2018, analysed and optimized method for mixed aleatory/epistemic uncertainties based on probability and evidence theory for excellent adaptability and reliability in the hull line design for achieving minimum EEDI [17].

Furthermore, adopting more efficient propulsion, such as fuel-saving engines or hybrid propulsion systems, significantly contributes to lowering the EEDI.

Transitioning to environmentally friendly fuels, such as LNG (Liquefied Natural Gas), and implementing good operational management practices, such as optimal route planning, can further improve energy efficiency. Routine maintenance of the vessel's engines and systems is also essential to ensuring optimal performance. By adopting this strategy, vessels can achieve substantial reduction in their EEDI, contributing to global emission reduction program. Technology for monitoring and data analysis can help optimize energy consumption and overall vessel performance. By adopting these strategies, vessels can significantly lower their EEDI and contribute to emission reductions effort. A similar study conducted by Prastowo H. et al. (2024) [18] analyzed the impact of vessel speed regulation on reducing the Carbon Intensity Indicator (CII) as a measure to lower GHG emissions. The study also considered the economic implications of changes in vessel speed, highlighting the balance between emission reduction and operational efficiency. The utilization of wind potential as an alternative energy source faces several limitations, such as fluctuations in wind speed, as noted by Suwarno et al. (2023) [19]. These limitations have driven numerous innovations in the implementation of sail technology, particularly in optimizing the shape and size of sails to enhance thrust and energy efficiency.

Studies related to the use of advanced sails have been conducted by several researchers. For example, Formosa et al., 2022 [20], examined the positive correlation between kite sail parameters and aerodynamic forces, demonstrating their impact on additional thrust. Similarly, Nyanya M et al., 2021 [21], explored the potential energy savings of up to 36% when rigid sails are positioned at the optimal angle. Research on rotors-based system has also been extensively conducted [22] focusing on optimizing rotor shape and their relationship to energy generation.

Studies by Suwarno et al. and Ismaiel A. et al. have concluded that rotor shape and dimensions significantly influence turbulence, which, in turn, affects the amount of power generated by the system. This article will explore the influence of rotor dimension parameters and environmental potential on reducing emissions, improving the Energy Efficiency Design Index (EEDI), and achieving energy savings across various ship sizes. This analysis is crucial for determining the optimal rotor dimensions for different ship sizes, tailored to the wind potential in specific regions.

This review is structured as follows. Section II explains the methodology, including the presentation of the rotor model, the ship lines plan for four DWT variations, and the EEDI calculation concept. Section III describes the post-processing of CFD results, providing analysis and visualization of numerical simulation data such as streamlines (visual representations of fluid flow patterns), fluid pressure distribution (indicating how pressure varies within a fluid or across a surface in a flow field), and pressure distribution on each rotor dimension at varying wind speeds. Section IV covers the verification and the validation of convergence plots from Computational Fluid Dynamics (CFD) simulations by using Ansys Fluent, showing residuals for various quantities during iterations.

Section V discusses rotor performance, detailing lift and drag for each model under different wind speed variations. Section VI elaborates on the comparison of EEDI for ships with and without sails. Finally, Section VII summarizes the review with some concluding remarks.

II. Methodology

II.1. Flowchart

This research focuses on optimizing ship design through the integration of rotor sails to reduce fuel consumption and CO_2 emissions. The analysis covers four ship sizes, ranging from 50,000 to 200,000 DWT, utilizing a combination of linear regression for main dimension calculations and resistance analysis. The study evaluates two primary design scenarios: ships equipped with rotor sails and ships without rotor sails. For the rotor sail configuration, three sail heights (20 meters, 25 meters, and 30 meters) are tested under varying wind velocities (5 m/s, 10 m/s, and 15 m/s). Computational modeling and meshing are performed to simulate aerodynamic effects, followed by power calculations. Post-processing includes the analysis of streamlines, lift, drag, and pressure data, which are subsequently used to determine the additional power requirements for vessels equipped with rotor sails.

For both scenarios, fuel oil consumption, CO_2 emissions, and the Energy Efficiency Design Index (EEDI) are calculated. Then a comparative analysis is conducted to evaluate the benefits of rotor sails in enhancing fuel efficiency and reducing emissions. The study concludes by discussing the feasibility and potential of rotor sails as a sustainable solution for improving the energy efficiency of ships.

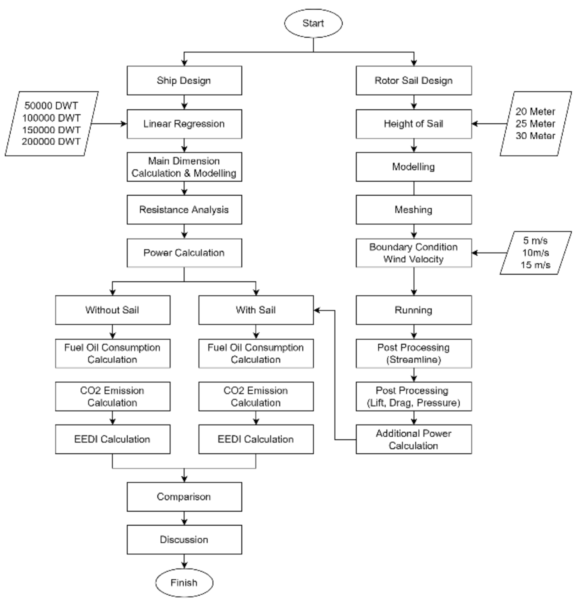

Fig. 1. Flowchart of Ship and Rotor Sail Design Process: from initial design calculations to final performance analysis and discussion

II.2. Sails Model

Rotor sails, leveraging the Magnus effect, enhance ship propulsion by harnessing wind energy. A comparison of three models with heights of 20 meters, 25 meters, and 30 meters reveals distinct advantages for each. The 20-meter model is optimal for smaller vessels and coastal operations due to its compact size and practicality. The 25-meter model strikes a balance between aerodynamic performance and structural considerations, making it versatile across various applications. The 30-meter model maximizes efficiency in open ocean conditions, making it the most suitable for larger vessels. Ultimately, selecting the appropriate rotor sail height depends on factors such as ship size, operational environment, and specific performance requirements.

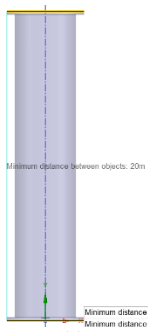

(a)

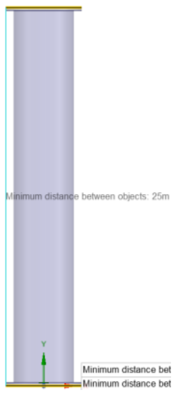

(b)

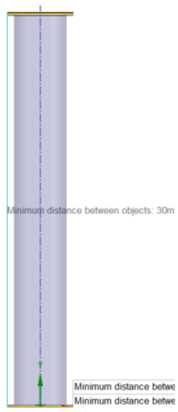

(c)

Figs. 2. Model of Rotor Sail (a) 20 Meter Height, (b) 25 Meter Height, (c) 30 Meter Height

II.3. Ships Model

A linesplan is a detailed drawing that provides both a profile and plan view of a ship's hull. It includes various curves, angles, and dimensions that define the vessel's hull shape, allowing naval architects and engineers to assess the ship's performance in water. The linesplan typically also includes information on the sheer, camber, and other essential structural details. This blueprint serves as a critical tool in ship design and construction [23].

II.4. Environment Condition

The image depicts a color-coded map representing the mean wind speed in Indonesia from 199 to 2009. The wind speeds are measured in meters per second, with the scale ranging from blue (representing lower speeds around -5 m/s) to red (indicating higher speeds up to around 15 m/s).

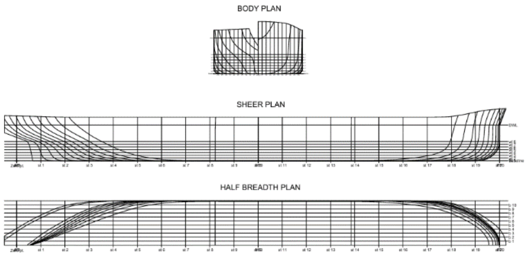

(a)

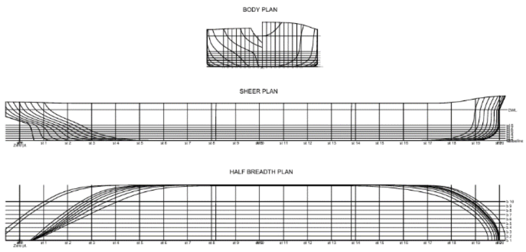

(b)

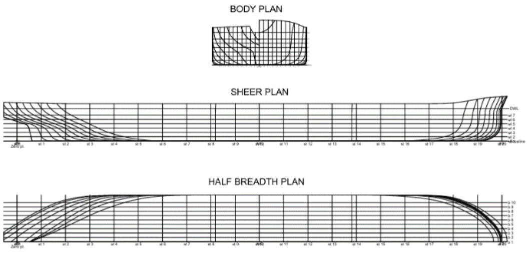

(c)

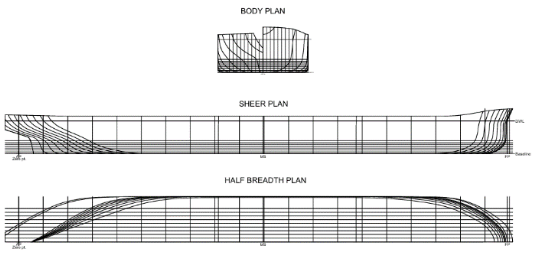

(d)

Figs. 3. Model Linesplan of Tanker (a) 50000 DWT, (b) 100000 DWT, (c) 150000 DWT, (d) 200000 DWT

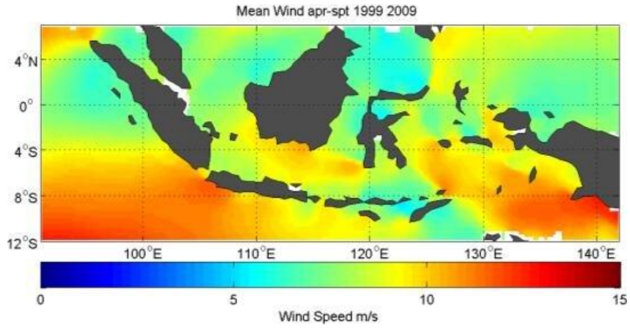

Fig. 4. Color-coded map of Indonesia showing mean wind speed from 1999 to 2009

The highest wind speeds are concentrated along the southern coastal regions and offshore areas, while lower wind speeds are observed inland and in northern areas [24].

II.5. EEDI Calculation

The Energy Efficiency Design Index (EEDI) is a measure of a ship's environmental impact, specifically regarding CO_2 emissions relative to the amount of cargo it transports. The formula for calculating the EEDI is generally expressed as [25]:

$$EEDI = \frac{\mathrm{CO_2\ emitted\ (g)}}{\mathrm{Deadweight\ (ton)} \times \mathrm{Distance\ Travelled\ (nm)}} \quad (1)$$

CO_2 Emissions are calculated based on the fuel consumption (FOC), as burning fuel oil produces a known amount of CO_2 per gram. Transport work is the product of the cargo carried (DWT in tons) and the distance travelled (in nautical miles), though distance is often standardized or simplified in design-stage calculations.

III. Post Processing

III.1. Streamline

In CFD (Computational Fluid Dynamics) post-processing, streamlines are visual representations of fluid flow patterns. They depict the trajectory that fluid particles follow, providing insights into the flow behavior around objects [32].

Streamlines help identify key features such as areas of high or low velocity, recirculation zones, and flow separation, making them essential for understanding complex fluid dynamics in simulations [26]. Figures 5 illustrate the velocity streamlines around the rotor sail.

III.2. Fluid Pressure Distribution

Fluid pressure distribution refers to how pressure varies within a fluid or across a surface in a flow field. It indicates the amount of force exerted by the fluid per unit area at different points.

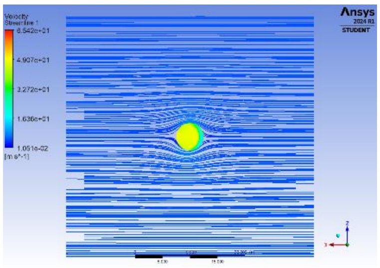

(a)

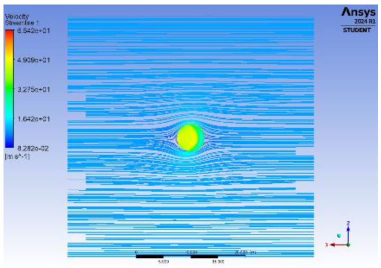

(b)

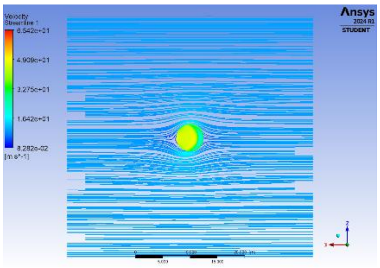

(c)

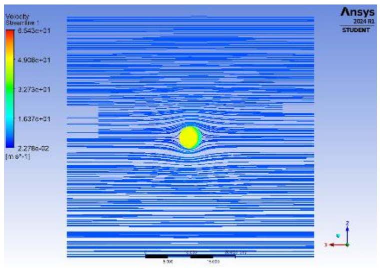

(d)

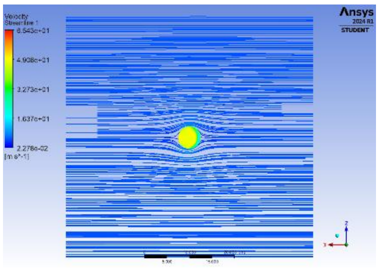

(e)

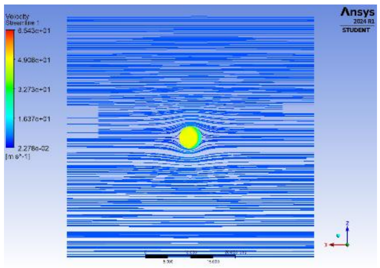

(f)

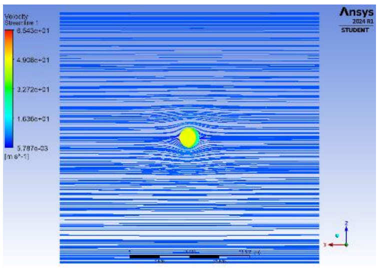

(g)

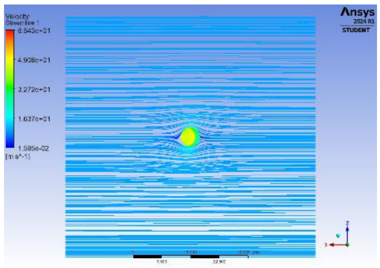

(h)

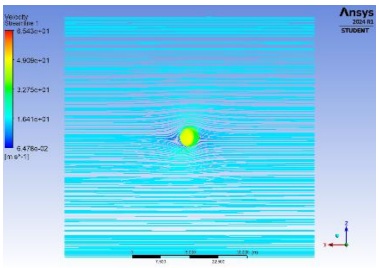

(i)

Figs. 5. Velocity Streamlines Around a Rotor Sail (a) Height 20 meter & Wind 5 m/s, (b) Height 20 meter & Wind 10 m/s (c) Height 20 meter & Wind 15 m/s, (d) Height 25 meter & Wind 5 m/s, (e) Height 25 meter & Wind 10 m/s (f) Height 25 meter & Wind 15 m/s, (g) Height 30 meter & Wind 5 m/s, (h) Height 30 meter & Wind 10 m/s (i) Height 30 meter & Wind 15 m/s

Factors affecting pressure distribution include fluid velocity, density, and external forces (like gravity). Understanding pressure distribution is crucial for analyzing fluid behavior, predicting forces on surfaces (like aircraft wings or pipes), and ensuring the structural integrity of engineering designs. It helps optimizing performance and safety in various applications [27]. Table I displays fluid pressure distribution at different wind velocities (5 m/s, 10 m/s, and 15 m/s) and rotor heights (20m, 25m, and 30m). As wind velocity increases, both minimum and maximum pressures become more negative, indicating heightened suction on the rotor. Higher rotor heights show similar trends, with slightly more negative minimum pressures and comparable maximum pressures [28]. Figures 6 present a visual of fluid pressure distribution around rotor sail.

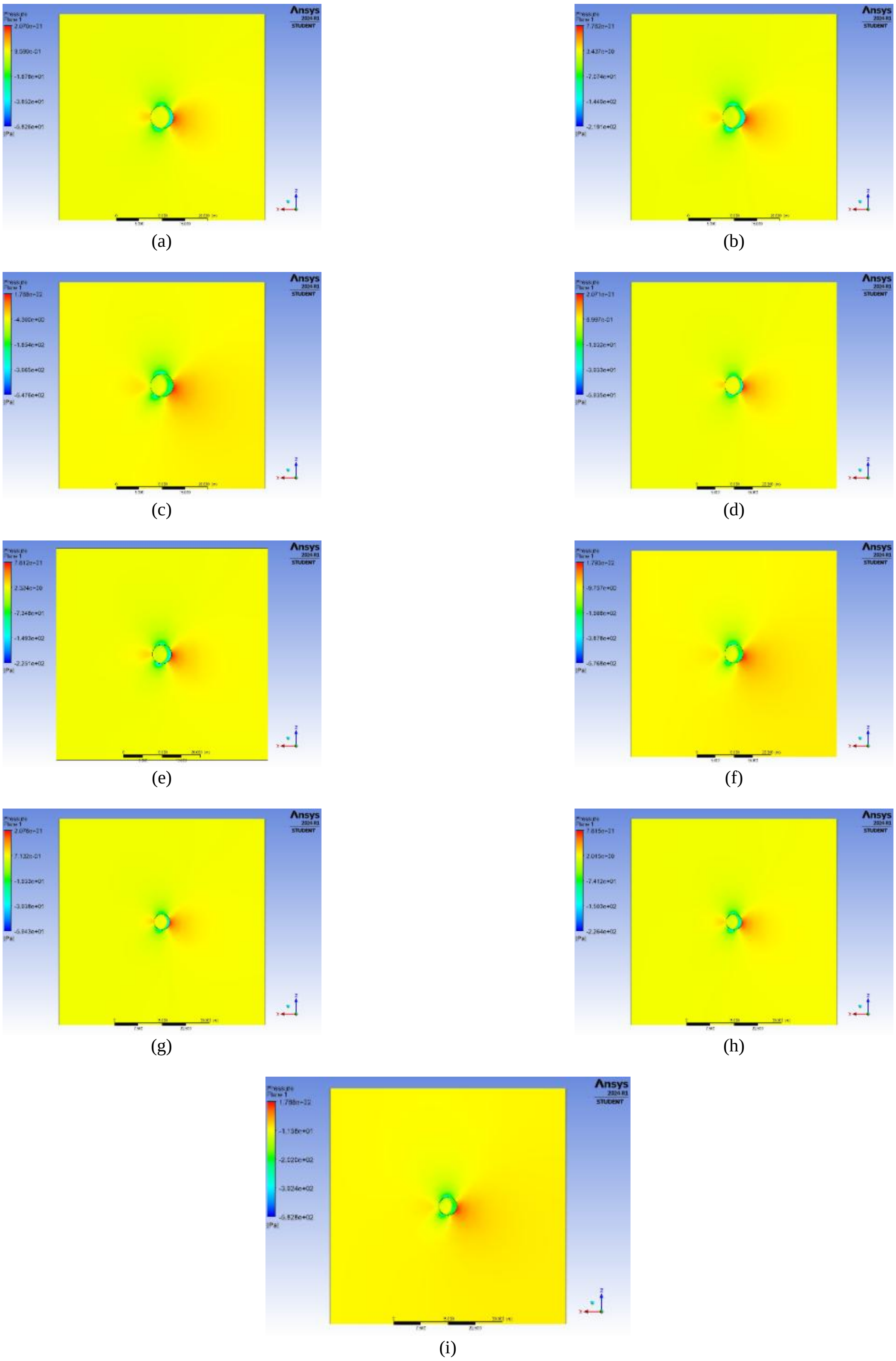

Figs. 6. Fluid Pressure Distribution Around a Rotor Sail (a) Height 20 meter & Wind 5 m/s, (b) Height 20 meter & Wind 10 m/s (c) Height 20 meter & Wind 15 m/s, (d) Height 25 meter & Wind 5 m/s, (e) Height 25 meter & Wind 10 m/s (f) Height 25 meter & Wind 15 m/s, (g) Height 30 meter & Wind 5 m/s, (h) Height 30 meter & Wind 10 m/s (i) Height 30 meter & Wind 15 m/s

III.3. Advance Sail Rotor Pressure Distribution

An advance sail rotor, or Flettner rotor, uses the Magnus effect to generate lift by creating a pressure differential around a spinning cylindrical structure mounted on a ship. Figures 7 explain the pressure distribution on each rotor dimension at varying wind speeds. The pressure distribution depends on the rotor's spin rate, wind speed, and direction. On the side where the cylinder rotates with the wind, the relative velocity increases, causing low pressure, while on the opposite side, where it rotates against the wind, high pressure forms. This pressure differential propels the vessel, and factors like rotor size and aerodynamic boundary layer also influence the rotor's efficiency [28].

TABLE I
PRESSURE DISTRIBUTION AT VARYING WIND VELOCITIES AND ROTOR HEIGHTS

Wind Velocity (m/s)	Rotor Height 20 Meter	Rotor Height 25 Meter	Rotor Height 30 Meter
5	Min -58.26 Pa Max 20.70 Pa	Min -59.35 Pa Max 20.71 Pa	Min -59.43Pa Max 20.76 Pa
10	Min -219.1 Pa Max 77.62 Pa	Min -225.1 Pa Max 78.12 Pa	Min -226.4 Pa Max 78.15 Pa
15	Min -547.6 Pa Max 176.8 Pa	Min -576.8 Pa Max 179.3 Pa	Min -582.8 Pa Max 178.8 Pa

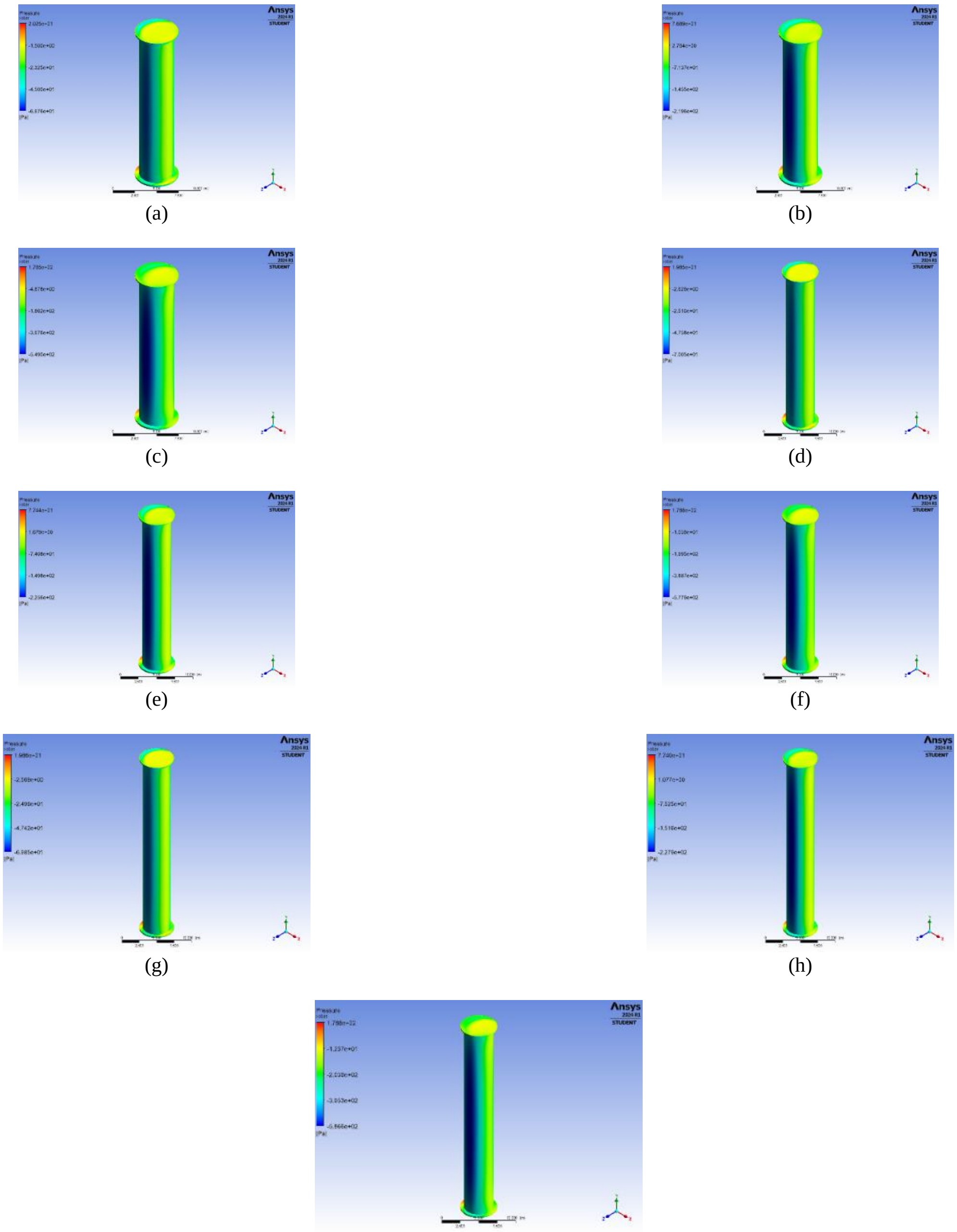

(a) (b) (c) (d) (e) (f) (g) (h) (i)

Figs. 7. Pressure Distribution on Rotor Sail (a) Height 20 meter & Wind 5 m/s, (b) Height 20 meter & Wind 10 m/s (c) Height 20 meter & Wind 15 m/s, (d) Height 25 meter & Wind 5 m/s, (e) Height 25 meter & Wind 10 m/s (f) Height 25 meter & Wind 15 m/s, (g) Height 30 meter & Wind 5 m/s, (h) Height 30 meter & Wind 10 m/s (i) Height 30 meter & Wind 15 m/s

TABLE II
PRESSURE CONTOUR DISTRIBUTION OF ROTOR SAIL ACROSS DIFFERENT WIND VELOCITIES AND ROTOR HEIGHTS

Wind Velocity (m/s)	Rotor Height 20 Meter	Rotor Height 25 Meter	Rotor Height 30 Meter
5	Min -66.76 Pa Max 20.25 Pa	Min -70.05 Pa Max 19.85 Pa	Min -69.85 Pa Max 19.86 Pa
10	Min -219.6 Pa Max 76.89 Pa	Min -225.6 Pa Max 77.44 Pa	Min -227.9 Pa Max 77.4 Pa
15	Min 549 Pa Max 176.5 Pa	Min -577.9 Pa Max 178.8 Pa	Min -586.6 Pa Max 178.8 Pa

Table II presents contour pressure distribution of sail at various wind velocities (5 m/s, 10 m/s, and 15 m/s) for rotor heights of 20 m, 25 m, and 30 m. As wind velocity increases, both minimum and maximum pressures become more negative, indicating greater suction effects on the rotor. Higher rotor heights generally show more negative minimum pressures, with maximum pressures remaining relatively stable across heights.

IV. Verification and Validation

IV.1. Residual Analysis

Figure 8 depicts a convergence plot from a Computational Fluid Dynamics (CFD) simulation by using Ansys Fluent, showing the residuals for various quantities over iterations. The X-axis represents the number of iterations, while the Y-axis displays residuals on a logarithmic scale, indicating the error remaining in the equations solved, with values ranging from 1 to 10-7.

Different colored lines represent residuals for continuity (cyan), X-velocity (blue), Y-velocity (orange), Z-velocity (green), turbulent kinetic energy (k, yellow), and specific dissipation rate (ω, red). The plot illustrates an initial high error that decreases as iterations progress, signalling improved solution accuracy, while periodic peaks may indicate computational adjustments like mesh updates or timestep changes [29].

V. Sail Performance

V.1. Lift and Drag

Table III outlines the drag and lift forces experienced by a rotor at various wind velocities (5 m/s, 10 m/s, and 15 m/s) and rotor heights (20 m, 25 m, and 30 m).

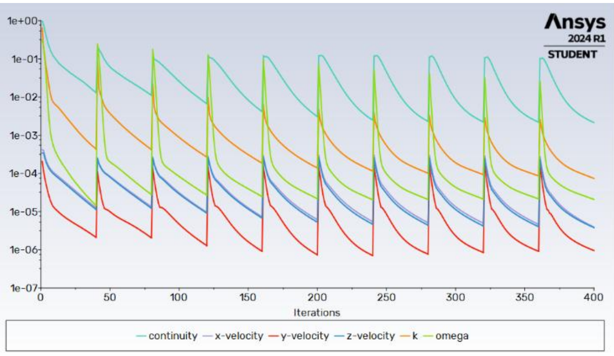

Fig. 8. Convergence history plot for Advance Sail CFD simulation

TABLE III
DRAG AND LIFT FORCE ON ROTOR AT VARYING WIND AND VELOCITIES

Wind Velocity (m/s)	Rotor Height 20 Meter	Rotor Height 25 Meter	Rotor Height 30 Meter
5	Lift 839.171 N Drag 2165.71 N	Lift 1021.94 N Drag 2761.86 N	Lift 1216.02 N Drag 3331.86 N
10	Lift 4586.45 N Drag 7300.06 N	Lift 5879.13 N Drag 9239.35 N	Lift 7111.11 N Drag 11166.7 N
15	Lift 18985.5 N Drag 19410.1 N	Lift 26203.7 N Drag 25307.3 N	Lift 32271.3 N Drag 30741 N

As wind velocity increases, both drag and lift forces rise significantly across all rotor heights. The data indicates that increasing the rotor height from 20m to 25m results in a 20% increase in lift and thrust forces, with a significant further increase observed as the rotor height continues to rise.

Notably, lift forces increase dramatically, indicating improved aerodynamic performance at higher velocities, while drag also rises but at a slower rate. Table IV presents the lift-to-drag ratios for a rotor at various wind velocities (5 m/s, 10 m/s, and 15 m/s) and rotor heights (20 m, 25 m, and 30 m). As wind velocity increases, the lift-to-drag ratio improves, indicating enhanced aerodynamic efficiency. Notably, the ratios are the highest at 15 m/s across all heights, suggesting better performance and effectiveness of the rotor design at higher wind speeds. This information is vital for optimizing rotor performance in wind turbines.

The fundamental aerodynamic principles that connect lift and drag forces on a rotor are influenced by several critical factors, such as the relative airflow velocity, air density, rotor dimensions, and the angle of attack. These principles are encapsulated in the basic aerodynamic equation, which demonstrates that both lift and drag forces increase quadratically with wind speed. This quadratic relationship underscores the significant impact of wind speed on rotor performance, as even small increases in wind velocity can result in disproportionately larger forces acting on the rotor.

Rotor height also significantly affects wind exposure, providing stronger and more stable airflow. Increasing the rotor height reduces ground-induced turbulence and drag, thereby enhancing aerodynamic efficiency. Raising the rotor height from 20 m to 25 m, and subsequently to 30 m, exposes the rotor to more stable wind flows, leading to a more substantial increase in lift force compared to drag force.

This phenomenon reflects an improvement in aerodynamic efficiency at higher wind speeds. This aligns with the research conducted by Guzelbulut [6]. Enhancing rotor height and operating at higher wind speeds can improve overall rotor performance, as observed in Tables III and IV.

TABLE IV
LIFT-TO-DRAG RATIO ON ROTOR AT VARYING WIND AND VELOCITIES

Wind Velocity (m/s)	Rotor Height 20 Meter	Rotor Height 25 Meter	Rotor Height 30 Meter
5	L/D 0.387	L/D 0.370	L/D 0.365
10	L/D 0.628	L/D 0.636	L/D 0.637
15	L/D 0.978	L/D 1.035	L/D 1.050

However, it is important to note that rotor design should also account for other factors, such as the structural loads caused by increased drag forces as conveyed by Kim [30].

Therefore, selecting strong yet lightweight materials is essential. Additionally, optimizing the angle of attack is a key strategy for maximizing lift forces while minimizing drag forces.

VI. EEDI Calculation

VI.1. Without Sail

Table V summarizes various performance metrics for different variations of vessels, including Deadweight Tonnage (DWT), power output (kW), Fuel Oil Consumption (FOC in tons), emitted CO_2 (in tons), and Energy Efficiency Design Index (EEDI). In general, ships with a larger DWT require higher power for operations, which automatically increases their fuel consumption.

However, it is observed that the Energy Efficiency Index (EEI) value decreases, indicating an improvement in energy efficiency. As DWT increases from A to D, power and FOC also rise, but the EEDI improves, indicating greater energy efficiency in larger vessels.

VI.2. With Sail

Table VI presents the Energy Efficiency Design Index (EEDI) for different vessel variations at three wind speeds (5 m/s, 10 m/s, and 15 m/s) along with their Deadweight Tonnage (DWT). As wind speed increases, the EEDI generally improves, indicating greater energy efficiency for all variations. Variation D consistently shows the lowest EEDI values, signifying the highest efficiency, while Variation A has the highest values. This information is essential for evaluating the energy performance and environmental sustainability of maritime vessels under varying wind conditions.

TABLE V
PERFORMANCE METRICS FOR VESSEL VARIATIONS: DWT, POWER, FOC, CO_2 EMISSIONS, AND EEDI WITHOUT SAIL

Variation	DWT	Power (kW)	FOC (ton)	Emitted CO_2 (ton)	EEDI
A	48620	4714	145	465	4.740
B	109307	7263	223	716	3.249
C	146726	9025	277	890	3.007
D	210707	10405	320	1026	2.414

TABLE VI
PERFORMANCE METRICS FOR VESSEL VARIATIONS: DWT, POWER, FOC, CO_2 EMISSIONS, AND EEDI WITH SAIL

Variation	DWT	Wind Velocity (m/s)	Power (kW)	FOC (ton)	CO_2 Emm. (ton)	EEDI
A	48620	5	4698	144	463	4.725
		10	4629	142	456	4.655
		15	4362	134	430	4.387
B	109307	5	7244	223	714	3.240
		10	7154	220	705	3.200
		15	6778	208	668	3.032
C	146726	5	9002	277	887	3.000
		10	8893	273	877	2.963
		15	8427	259	831	2.808
D	210707	5	10382	319	1023	2.409
		10	10273	316	1013	2.384
		15	9807	302	967	2.276

The comparison between ships without sails and those with rotor sail applications demonstrates significant improvements in energy efficiency, evidenced by a reduction in fuel consumption and CO_2 emissions. For ships with larger DWT, the fuel savings improve, particularly at higher wind speeds. This can be understood as a correlation between the increased lift and thrust forces on the ship, as shown in Table III.

VI.3. Comparison

Table VII indicates that incorporating sails significantly enhances the energy efficiency of maritime vessels, as reflected in the consistently lower Energy Efficiency Design Index (EEDI) values across all variations and wind speeds (5 m/s, 10 m/s, and 15 m/s).

The improvements are particularly notable at higher wind speeds, demonstrating the effectiveness of sail assistance. Variation D emerges as the most efficient option, displaying the lowest EEDI values when sails are used. While all the variations benefit from this technology, larger vessels like Variation D experience more substantial efficiency gains. Overall, these findings underscore the potential of sail-assisted designs to reduce emissions and promote sustainability in maritime operations, especially under favorable wind conditions.

As is well known, the regulatory demands set by the IMO regarding the environmental impact of maritime operations are becoming increasingly stringent. The Energy Efficiency Design Index (EEDI) has become a critical parameter in the maritime industry for measuring the energy efficiency of ships, particularly greenhouse gas emissions per unit of transport. Increased wind speeds significantly enhance the contribution of wind-assisted power in overcoming the ship's resistance. This results in reduced fuel consumption, leading to a decrease in EEDI values, as shown in Table VI.

The reduction in EEDI at higher wind speeds reflects an improvement in the ship's energy efficiency, in line with the results of the research conducted by Ammar [31]. The influence of key ship design factors, particularly at different Deadweight Tonnages (DWT), also plays a significant role in EEDI values. Ships with higher DWT tend to demonstrate better efficiency due to their larger cargo capacity, which reduces emissions per ton of cargo transported. EEDI is a key indicator supporting global initiatives to reduce the carbon footprint of maritime transportation.

A lower EEDI value not only signifies reduced carbon emissions but it also indicates lower operational costs due to decreased fuel consumption. The use of sail technology significantly improves the energy efficiency of vessels, providing a viable solution for enhancing maritime performance.

Notably, the Energy Efficiency Design Index (EEDI) decreases with the application of sails across various vessel types and wind speeds, indicating a clear correlation between sail utilization and improved efficiency.

TABLE VII
EEDI COMPARISON FOR VESSEL VARIATIONS WITH AND WITHOUT SAIL ASSISTANCE AT DIFFERENT WIND SPEEDS

Variation	DWT	EEDI without Sail	EEDI with Sail 5 m/s	EEDI with Sail 10 m/s	EEDI with Sail 15 m/s
A	48620	4.740	4.725	4.655	4.387
B	109307	3.249	3.240	3.200	3.032
C	146726	3.007	3.000	2.963	2.808
D	210707	2.414	2.409	2.384	2.276

Furthermore, efficiency gains are the most pronounced at higher wind speeds, displaying the additional benefits of integrating sails in favorable wind conditions.

Additionally, larger vessels demonstrate greater efficiency gains when employing sail technology, underscoring its effectiveness for bigger ships. Collectively, these findings highlight the substantial potential of sail technology to reduce emissions and enhance the sustainability of maritime operations, making it a promising avenue for environmentally friendly shipping practices.

VII. Conclusion

The study on the use of advanced rotor-type sails for EEDI on ships with various DWT types is a critical aspect of advancing green technology interventions in the maritime sector. This effort aims to enhance energy efficiency and reduce emissions to achieve the 2050 zero-carbon target. The initial stage involves modeling rotors and ships with varying dimensions, tested under different wind speeds using computational fluid dynamics to assess the energy performance generated by the rotors. A comparison of results before and after rotor implementation in EEDI calculations becomes the ultimate objective of this study. The review has yielded several interesting conclusions. The use of rotors on large ships shows a significant reduction in fuel consumption, especially at higher wind speeds, along with a notable decrease in CO_2 emissions. A clear correlation is observed between the improvement in the Energy Efficiency Design Index (EEDI), wind speed, rotor dimensions, and ship size.

The findings provide tangible evidence of the positive potential of rotor sails as an auxiliary power solution across various ship size variations. Although the potential EEDI improvement is more pronounced in larger DWT ships than in smaller ones, this holds true under the same rotor dimensions and wind speed conditions. The application of rotors as a supplementary energy source is vital for shipowners amid efforts to save energy, transition from fossil fuels, comply with increasingly stringent emission regulations, and achieve global emission reductions. Further research is necessary to enhance the energy potential generated by rotors. This can be achieved through rotor redesign simulations, exploring rotational combinations, experimental validation by using towing tunnels, and ultimately developing optimal rotor designs tailored to specific ship dimensions and environmental conditions of the operational waters.

Acknowledgements

We express our gratitude to The Ministry of Education, Culture, Research, and Technology KEMDIKBUDRISTEK of Indonesia for funding this research through BIMA 2024. Grant contract number 109/E5/PG.02.00.PL/2024.

References

[1] S. Al Mamun, Z. I. Chowdhury, M. S. Kaiser, and M. S. Islam, Techno-financial analysis and design of on-board intelligent-assisting system for a hybrid solar–DEG-powered boat, *Int. J. Energy Environ. Eng.*, vol. 7, no. 4, pp. 361–376, 2016. doi: 10.1007/s40095-016-0218-0

[2] H. Johnson, M. Johansson, and K. Andersson, Barriers to improving energy efficiency in short sea shipping: An action research case study, *J. Clean. Prod.*, vol. 66, 2014. doi: 10.1016/j.jclepro.2013.10.046

[3] P. Napolitano, V. Fraioli, C. Guido, and C. Beatrice, Assessment of optimized calibrations in minimizing GHG emissions from a Dual Fuel NG/Diesel automotive engine, *Fuel*, vol. 258, 2019. doi: 10.1016/j.fuel.2019.115997

[4] IMO, Fourth IMO Greenhouse Gas Study 2020 - Executive Summary, *Int. Marit. Organ.*, vol. 1, no. 69, 2021.

[5] IMO, Third IMO Greenhouse Gas Study 2014, *Int. Marit. Organ.*, 2014, doi: 10.1007/s10584-013-0912-3

[6] C. Guzelbulut and K. Suzuki, Optimal Design of Rotor Sails Based on Environmental Conditions and Cost, *J. Mar. Sci. Eng.* 2024, Vol. 12, Page 31, vol. 12, no. 1, p. 31, Dec. 2023. doi: 10.3390/jmse12010031

[7] Saavedra, A., Galvis, N., Mesa, F., Banguero, E., Castaneda, M., Zapata, S., Aristizabal, A., Current State of the Worldwide Renewable Energy Generation: a Review, (2021) *International Journal on Engineering Applications (IREA)*, 9 (3), pp. 115-127. doi: https://doi.org/10.15866/irea.v9i3.19987

[8] S. H. Dolatabadi, A. I. Ölçer, and S. Vakili, The Application of Hybrid Energy system (Hydrogen Fuel cell, wind, and solar) in shipping, *Renew. Energy Focus*, vol. 46, pp. 197–206, Sep. 2023. doi: 10.1016/j.ref.2023.05.008

[9] T. Tuswan et al., Representative application of LNG-fuelled ships: a critical overview on potential GHG emission reductions and economic benefits, *Brodogradnja*, vol. 74, no. 1, pp. 63–83, 2023. doi: 10.21278/brod74104

[10] Ariani, B., Ariana, I., Fathallah, A., Experimental Investigation on Natural Gas Injection to Minimize Abnormal Combustion and Methane Slip in the Diesel - Natural Gas Dual Fuel Engine at Low Load, (2020) *International Review of Mechanical Engineering (IREME)*, 14 (9), pp. 599-606. doi: https://doi.org/10.15866/ireme.v14i9.19821

[11] A. D. Korberg, S. Brynolf, M. Grahn, and I. R. Skov, Techno-economic assessment of advanced fuels and propulsion systems in future fossil-free ships, *Renew. Sustain. Energy Rev.*, vol. 142, p. 110861, May 2021. doi: 10.1016/j.rser.2021.110861

[12] H. Xing, C. Stuart, S. Spence, and H. Chen, Alternative fuel options for low carbon maritime transportation: Pathways to 2050, *J. Clean. Prod.*, vol. 297, p. 126651, May 2021. doi: 10.1016/j.jclepro.2021.126651

[13] D. Li, G. Li, J. Dai, and P. Li, A new type of collapsible wing sail and its aerodynamic performance, *Proc. Int. Conf. Offshore Mech. Arct. Eng. - OMAE*, vol. 10, 2017. doi: 10.1115/omae2017-61084

[14] M. S. Çalışal, O. Yurdakul, G. N. Küçüksu, and A. Z. Saydam, A Decision Making Process for the Selection of Better Ship Main Dimensions with the Fuel EEDI Requirements, *SNAME 14th Int. Mar. Des. Conf. IMDC 2022*, Jun. 2022. doi: 10.5957/imdc-2022-226

[15] Y. H. Hou, X. Liang, and X. Y. Mu, Hull Lines Reliability-Based Optimisation Design For Minimum EEDI, *Brodogr. An Int. J. Nav. Archit. Ocean Eng. Res. Dev.*, vol. 69, no. 2, pp. 17–33, Jun. 2018.

doi: 10.21278/brod69202
[16] H. Ren, Y. Ding, and C. Sui, Influence of EEDI (Energy Efficiency Design Index) on Ship–Engine–Propeller Matching, *J. Mar. Sci. Eng.* 2019, Vol. 7, Page 425, vol. 7, no. 12, p. 425, Nov. 2019. doi: 10.3390/jmse7120425
[17] Y. hang Hou, Y. jia Li, and X. Liang, "Mixed aleatory/epistemic uncertainty analysis and optimization for minimum EEDI hull form design," *Ocean Eng.*, vol. 172, pp. 308–315, Jan. 2019. doi: 10.1016/j.oceaneng.2018.12.003
[18] Prastowo, H., Pitana, T., Artana, K., Ariana, I., Evaluation of Carbon Intensity Index for Ship with Recommended Actions to Improve CII Rating, (2024) *International Review of Mechanical Engineering (IREME)*, 18 (5), pp. 247-255. doi: https://doi.org/10.15866/ireme.v18i5.24825
[19] Suwarno, S., Cahyadi, C., Sukarwoto, S., Dewi, A., Pinayungan, D., Comparative Analysis of Wind Speed and Energy Potential Assessment of Two Distribution Models in Medan, Indonesia, (2023) *International Review of Electrical Engineering (IREE)*, 18 (4), pp. 275-282. doi: https://doi.org/10.15866/iree.v18i4.22725
[20] W. Formosa, T. Sant, C. D. M. Muscat-Fenech, and M. Figari, Wind-Assisted Ship Propulsion of a Series 60 Ship Using a Static Kite Sail, *J. Mar. Sci. Eng. 2023*, Vol. 11, Page 117, vol. 11, no. 1, p. 117, Jan. 2023. doi: 10.3390/jmse11010117
[21] M. N. Nyanya, H. B. Vu, A. Schönborn, and A. I. Ölçer, Wind and solar assisted ship propulsion optimisation and its application to a bulk carrier, *Sustain. Energy Technol. Assessments*, vol. 47, no. June, 2021. doi: 10.1016/j.seta.2021.101397
[22] A. De Marco, S. Mancini, C. Pensa, R. Scognamiglio, L. Vitiello, Marine application of flettner rotors: Numerical study on a systematic variation of geometric factor by doe approach, in *International Conference on Computational Methods in Marine Engineering*, 2015.
[23] A. Papanikolaou, Naval Architectural Drawings and Plans, *Sh. Des.*, pp. 359–391, 2014. doi: 10.1007/978-94-017-8751-2_4
[24] H. P Dida, S. Suparman, and D. Widhiyanuriyawan, Pemetaan Potensi Energi Angin di Perairan Indonesia Berdasarkan Data Satelit QuikScat dan WindSat (Mapping Wind Energy Potential in Indonesian Waters Based on QuikScat and WindSat Satellite Data), *J. Rekayasa Mesin*, vol. 7, no. 2, pp. 95–101, Aug. 2016. doi: 10.21776/ub.jrm.2016.007.02.7
[25] S. S. Lee, Analysis of the effects of EEDI and EEXI implementation on CO2 emissions reduction in ships, *Ocean Eng.*, vol. 295, p. 116877, Mar. 2024. doi: 10.1016/j.oceaneng.2024.116877
[26] B. Ariani, Febriyan, D. Sholahudin, A. C. Nagra, M. Oktaviani, and M. H. Hakim, Investigating Airflow Patterns in the XYZ Passenger Ship's Accommodation Room on the Potential for COVID-19 Exposure to Passengers, *IOP Conf. Ser. Earth Environ. Sci.*, vol. 1250, no. 1, 2023. doi: 10.1088/1755-1315/1250/1/012006
[27] S. Guntur and N. N. Sørensen, A study on rotational augmentation using CFD analysis of flow in the inboard region of the MEXICO rotor blades, *Wind Energy*, vol. 18, no. 4, pp. 745–756, Apr. 2015. doi: 10.1002/WE.1726
[28] J. Li, H. Lin, C. Sun, B. Jiao, G. Sun, and F. Cao, Analysis of Aerodynamic Performance and Application of Flettner Rotor, *J. Inst. Eng. Ser. C*, pp. 1–11, Aug. 2024. doi: 10.1007/s40032-024-01073-9/metrics
[29] F. Stern et al., *Verification And Validation Of CFD Simulations*, IIHR Report No. 407.
[30] D. M. Kim, S. H. Hong, S. H. Jeong, and S. J. Kim, Analysis of Dynamic Characteristics of Rotor Sail Using a 4DOF Rotor Model and Finite Element Model, *J. Mar. Sci. Eng.* 2024, Vol. 12, Page 335, vol. 12, no. 2, p. 335, Feb. 2024. doi: 10.3390/JMSE12020335
[31] N. R. Ammar and I. S. Seddiek, Wind assisted propulsion system onboard ships: case study Flettner rotors, *Ships Offshore Struct.*, vol. 17, no. 7, pp. 1616–1627, Jul. 2022. doi: 10.1080/17445302.2021.1937797
[32] Kunjappan, J., Prakash, A., Computational Fluid Dynamics Study of Aircraft Wing with Winglet Performance at High Subsonic Speeds, (2022) *International Review of Aerospace Engineering (IREASE)*, 15 (5), pp. 254-261. doi:https://doi.org/10.15866/irease.v15i5.22870

Authors' information

[1]Department of Naval Architecture, Faculty of Engineering, Universitas Muhammadiyah Surabaya, Surabaya, Indonesia.

[2]Department of Mechanical Engineering, Faculty of Engineering, Universitas Muhammadiyah Surabaya, Surabaya, Indonesia.

[3]PT PAL Indonesia, Surabaya, Indonesia.

Betty Ariani was born in east java, Indonesia on 17th December 1979. She received doctoral programme from Institut Teknologi Sepuluh Nopember (ITS) Surabaya, Indonesia, in Marine Technology. Her current research focused on fuel technology and renewable energy, marine power plant and emission control technology. Mrs. Betty is researcher and lecturer in Universitas Muhammadiyah Surabaya since 2013.

Ponidi was born in East Java, Indonesia on 3th February 1972. Currently he is focusing on conducting research on CO_2 Capture and Storage (CCS) using environmentally friendly membrane technology. Mr. Ponidi has been a researcher and lecturer at the Muhammadiyah University of Surabaya since 1997 and a Doctoral candidate at the Department of Mechanical Engineering in the field of energy conversion engineering, Brawijaya University Malang, Indonesia. Apart from being a lecturer, he is also a team of experts in the field of shipping machinery and construction

Moh. Arif Batutah was born in east java, Indonesia on 6th June 1974. He received Doctor degree programme from Institut Teknologi Sepuluh Nopember (ITS) Surabaya, Indonesia, in Process Technology and System Engineering. His current research focused on biodiesel fuel and renewable energy. Mr. Batutah is researcher and lecturer of Mechanical Engineering in Universitas Muhammadiyah Surabaya since 2014.

Ardan Nagra Coutsar was born in east java, Indonesia on Desember 1996. He received Master degree programme from Republic of Indonesia Defense University, Indonesia, in Faculty of Defense Science and Technology. His current research focused on numerical study such as Computational Fluid Dynamics (CFD) and Finite Element Method (FEM). Apart from being a researcher in Universitas Muhammadiyah Surabaya, he is also as design engineer in PT PAL Indonesia.